Dst model for 1995–2002

M. Temerin[1] and Xinlin Li[2]

Received 6 June 2005; revised 4 January 2006; accepted 10 January 2006; published 29 April 2006.

[1] The *Dst* index is predicted on the basis of the solar wind for the years 1995–2002 using an update of the previous Temerin and Li [2002] prediction model for *Dst*. The updated model is based on additional data from the years 2000–2002 corresponding to the maximum of the solar cycle and includes several large magnetic storms. For this 8-year period, the linear correlation between the model and the *Dst* index is 0.956, the prediction efficiency is 0.914, and the RMS error of the prediction is 6.65 nT (nanoTesla). An analysis of some of the error in the model indicates that at least 25% of the remaining error is due to the effect on the *Dst* index of a portion of the Sq ionospheric current system and that close to 99% of the variance of *Dst* index due to magnetospheric currents is predictable. An examination of 10-day intervals around the six largest magnetic storms for which there is good solar wind data shows prediction efficiencies between 0.93 and 0.98 and linear correlation coefficients between 0.96 and 0.99. It is suggested that the annual variation in the *Dst* index is mainly due to magnetopause and ring currents and the location of the magnetometer stations used to calculate the *Dst* index. The dependence of the model on the solar wind implies that magnetospheric activity depends on the solar wind approximately in proportion to the square root of the density, square of the velocity, and linearly with the interplanetary magnetic field (IMF). In addition, there is strong dependence on the direction of IMF such that magnetic activity depends approximately on the sixth power of the sine of half the IMF clock angle, where the IMF clock angle is angle of the IMF in the plane perpendicular to the solar wind velocity measured from the northward direction. The model has also strong dependence on the angle between the dipole axis and the solar wind velocity which explains, in part, the seasonal dependence of magnetospheric activity. Overall, the updated model further demonstrates that the large-scale currents that affect the *Dst* index are well controlled by solar wind variations.

Citation: Temerin, M., and X. Li (2006), *Dst* model for 1995–2002, *J. Geophys. Res.*, *111*, A04221, doi:10.1029/2005JA011257.

1. Introduction

[2] Here we provide an updated version, based on solar wind data from the years 1995–2002, of our *Dst* model [*Temerin and Li*, 2002]. The previous version was based on nearly 5 years (1995–1999) of almost continuous solar wind and *Dst* data. The solar wind during the years 1995–1999 was relatively tame: The solar wind speed only twice reached 900 km/s, and the z-component (in GSM coordinate) of interplanetary magnetic field, Bz, never fell below -30 nT (from data with a 10-min cadence), versus 4 times when the velocity exceeded 900 km/s and 7 times when Bz fell below −30 nT for the years 2000–2002. The solar wind data were, at first, from the WIND spacecraft [*Lin et al.*, 1995; *Lepping et al.*, 1995] and then combined with solar wind data from ACE spacecraft [*Smith et al.*, 1999; *McComas et al.*, 1998] after its launch in 1998 to fill gaps in the WIND data. Since 2000, we have been using the data exclusively from ACE. All solar wind data were propagated to the magnetosphere (see Appendix A for details). Thus here we report the results of our updated model for the 8 years 1995–2002 (the final *Dst* for 2003 is not available as of this report) and the changes we have made in our model. The 5 years 1995–1999 included part of the declining phase of last solar cycle in 1995, the solar cycle minimum in 1996–1997, and the ascending phase of this solar cycle in 1998–1999. The additional years 2000–2002 include the solar maximum of the current solar cycle and thus the model is now based on various solar wind conditions in different phases of the solar cycle.

[3] The changes we have made in our model fall into three categories. The first category of changes is an update of the parameters in the model to include the new solar wind and *Dst* data. The second category includes somewhat technical changes in the model to accommodate more extreme solar wind data. The previous version failed in two cases during the years 2000–2002 because of division by practically zero in one case and because of a change in the sign of the driver term in another case. The third

[1]Space Sciences Laboratory, University of California, Berkeley, Berkeley, California, USA.
[2]Laboratory for Atmospheric and Space Physics, University of Colorado, Boulder, Colorado, USA.

Copyright 2006 by the American Geophysical Union.
0148-0227/06/2005JA011257$09.00

category includes changes to explore new physics or to try to explain existing peculiarities in the model. While these last changes as a whole only slightly improve the model, they provide some additional insight into the behavior of *Dst* and of the magnetosphere. These latter changes also required an additional update of the parameters. Appendix A describes all the details of model for those who wish to learn it in detail, reproduce it, use it, or improve it (the source codes of this model are available upon request). In the main text we provide an outline of the model, display its behavior, and comment on the physical significance of the model.

[4] For this 8-year period the linear correlation coefficient, LC, between the model and the *Dst* index is 0.956, the prediction efficiency, PE, (PE = [1-(mean squared residual)/(variance of data)], where the residual is the difference between the data and the prediction) is 0.914, and the RMS error of the prediction is 6.65 nT. In the previous model for the years 1995–1999 the respective values were 0.94, 0.88 and 6.4 nT. The PC and LC are now better even though the RMS error is larger. This is because of the larger variance of the *Dst* index during the years 2000–2002.

2. Model Description

[5] Our modeled *Dst* is a sum of the following six terms:

$$Dst = dst1* + dst2* + dst3* + (pressure\ term)* + (direct\ IMF\ Bz\ term)* + (offset\ terms). \quad (1)$$

The terms *dst*1, *dst*2, *dst*3, (*pressure term*), and (*direct Bz term*) were all in our previous model [*Temerin and Li*, 2002]. The terms *dst*1*, *dst*2*, *dst*3*, (*pressure term*)*, (*direct Bz term*)* differ, in part, from our previous model in that they now incorporate an annual variation. The detailed formula are listed in Appendix A.

[6] The parameters in the model are found by minimizing the RMS error between the prediction and the *Dst* index. This has been done mostly "by hand." That is, a single parameter is changed slightly and 8 years of data is run (this takes about 40 s on a PC). If the RMS error is reduced this parameter is adopted as the new best parameter. This procedure is iterated over all the parameters many times to find a better set of parameters. We also sometimes experiment with changes in the algorithm which require further changes in the parameters. After doing this for a couple years in our spare time we have come up with the current set of best parameters.

[7] There are predictions of *Dst* that use the current known value to predict the next value. Our model, however, does not use any known values of *Dst* to make predictions of *Dst*. Past known values of *Dst* are not an input to the model. The only input to the model is the solar wind. All terms in the model except the offset term depend only on the solar wind. The *dst*1, *dst*2, and *dst*3 terms all have a driver term and a decay term and are calculated in a similar way: $dstx(t + dt) = dstx(t) + (driver\ term) - (decay\ term)$ (x = 1, 2, 3). There is a threshold for *dst*1 to have any growth, similar to the Burton formula [*Burton et al.*, 1975]. However, the *dst*2 and *dst*3 terms have no thresholds.

[8] The driver terms are a function of the current values of the solar wind magnetic field, density, and velocity and of the past values of the solar wind magnetic field and of past values of *dst*1 and *dst*2. The driver terms determine how the solar wind controls the *Dst* index and, to the extent that changes in *Dst* index reflect magnetospheric activity, how the solar wind controls the magnetosphere. While the individual driver terms have somewhat different dependencies on the solar wind parameters the general pattern is as follows: The driver terms depend on the solar wind density approximately as the square root of the density, depend on the solar wind velocity approximately as the square or slightly higher power of the solar wind velocity, and depend on the magnitude of IMF approximately linearly. This dependence, approximately expressed as Ey*(dynamic pressure)$^{0.5}$, is close to the dependence on these parameters of the transpolar potential when it is in saturation [*Siscoe et al.*, 2002].

[9] The *dst*1 and *dst*2 have a stronger dependence on velocity than the *dst*3 term. Why this is so is not clear but in any case the *dst*3 contribution is smaller than the *dst*1 and *dst*2 contributions which thus dominate the overall response of the model to the solar wind velocity. In contrast some simpler models [e.g., *Burton et al.*, 1975] have a linear dependence on the solar wind electric field which is equivalent to a linear dependence on the solar wind velocity.

[10] The importance of the IMF in determining magnetospheric activity is well known. In some models [e.g., *Burton et al.*, 1975] only the Bz component is used: a large southward IMF produces strong activity. A slightly more subtle dependence is given by using the IMF clock angle which depends on the ratio of the Bz and By components of the IMF. A linear dependence on the magnitude of the IMF in the Bz-By plane and a dependence on the fourth power of the sine of half the IMF clock angle was associated with magnetospheric activity by [*Perreault and Akasofu*, 1978]. We also use the magnitude of the IMF in Bz-By plane and the clock angle for the driver terms. We find almost a linear dependence on the magnitude of the IMF in Bz-By plane but a stronger dependence on the clock angle: about a power of 6 in the sine term instead of 4. Our model also includes a dependence on the angle of the IMF in the By-Bx plane. The net result of fitting the dependence of the driver terms on this angle is to show that the driver terms have practically no dependence on the Bx component but an additional, not well understood, dependence on the IMF By component and the angle of the dipole tilt.

[11] The driver terms also have a strong dependence on the angle between the solar wind velocity and Earth's magnetic dipole axis such that the strongest drivers occurs when the dipole axis is perpendicular to the solar wind velocity. This angle determines, in part, the seasonal dependence of magnetic activity and of the *Dst* index [*Cliver et al.*, 2000; *Li et al.*, 2001a].

[12] The *dst*1 driver term also has a dependence on previous values of *dst*1 and *dst*2 while the *dst*2 driver term has a dependence on the previous values of *dst*1. The effect of these terms is to limit the growth of *dst*1 and *dst*2 if *dst*1 or *dst*2 were large in the recent past. In this revised model the driver terms also depend on past values of the IMF Bz component. The rationale for this addition is described in Appendix A.

[13] The *dst*1, *dst*2, and *dst*3 terms differ most strongly in their decay rates. The *dst*1 and *dst*2 terms have nonlinear

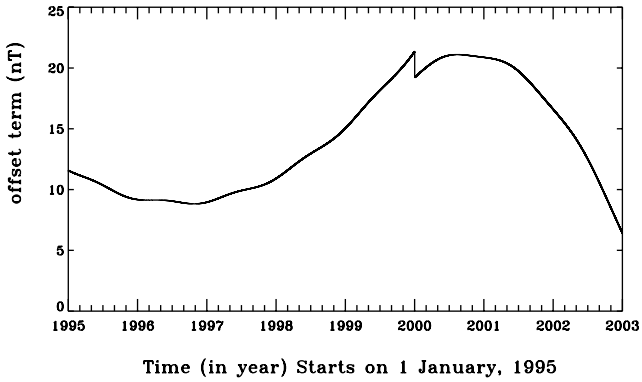

Figure 1. Magnitude of offset term as a function of time for the eight years 1995–2002. The discontinuity at the end of 1999 is due to the fact that we did two separate quadratic fits for the years 1995–1999 and the years 2000–2002 (see Appendix A for details).

decay rates that increase with the magnitude of the respective terms. The decay rate of the *dst*3 however term is only weakly dependent on its amplitude. The typical decay time of the *dst*1 term is several days; the typical decay time of the *dst*2 term is a day; and the typical decay time of the *dst*3 of about 5 hours. These *dst*1, *dst*2, and *dst*3 terms can be interpreted as representing three current systems within the magnetosphere that contribute to *Dst*: the classic ring current (trapped ions within the dipole-like field of the Earth), the so-called partial ring current, and perhaps the magnetotail current, respectively. The physical interpretation of *dst*3 term we regard as more uncertain.

[14] The pressure term and the direct IMF Bz term are calculated directly from the solar wind. The *Direct IMF Bz term* is a small term with an average magnitude of about half the IMF Bz or 1–2 nT. It has a strong dependence on the angle of the dipole with respect to the solar wind velocity. It suggests that a portion of the IMF penetrates directly to the surface of the Earth. However, this is not well understood.

[15] The *pressure term* is usually taken [e.g., *Burton et al.*, 1975] to be proportional to the square root of the dynamic pressure of the solar wind, $(nv^2)^{\frac{1}{2}}$, where n is the solar wind density (cm^{-3}) and v is the solar wind velocity (km/s). This term is usually assumed to represent magnetopause and solar wind currents. Our model, however, has an additional IMF magnetic pressure and solar wind density term. To further explore the behavior of this term we have now added an expression proportional to b^2*n, which was not in previous model. However, adding this term improved the fit and so we kept it thus further complicating the overall "pressure" term.

[16] The "offset term" may compensate for a portion of the secular variation that may not have been removed in calculating the *Dst* index. It also compensates, in part, for the annual variation in *Dst*. The offset term is shown is Figure 1. The offset term consists of a constant and a linear and a quadratic function of time and a sine term with an annual period. Because we did two separate quadratic fits for the years 1995–1999 and the years 2000–2002, there is a discontinuity at the end of 1999. The *Dst* index is adjusted for the secular variation of the Earth's main internal magnetic field. Currently, this field is decaying. The adjustment is done by doing a quadratic fit to 5 years of magnetometer data using quiet days. In the absence of the offset term the model would predict a more negative *Dst* during solar maximum than the "Kyoto" *Dst* index. We are uncertain whether this is because the rest of the model does not predict magnetospheric activity correctly as a function of solar cycle or whether this is because, in adjusting for the secular variation, the "Kyoto" *Dst* index also removes real magnetospheric effects. A further interesting discussion of possible *Dst* index errors is given by *Karinen and Mursula* [2005].

[17] The *Dst* index has an annual variation in addition to the larger and better known semi-annual variation. The semi-annual variation reflects the enhanced magnetic activity during the equinoxes. The annual variation produces a more positive *Dst* index during the late Northern Hemisphere spring. In our previous version the annual variation was included as a sine wave in the offset term with an amplitude of 1.44 nT. The best fit for the years 1995–2002 gives an even larger amplitude of 3.2 nT in the absence of other changes in the model.

[18] To investigate the origin of the annual variation we have included an annual modulation in all the six terms of our model. The result is that the annual variation is dominated by the annual variation of the pressure and the dst1 terms. The pressure term has about a 10% annual variation while the dst1 term has about an 8% annual variation. Only a small residual annual variation with an amplitude of 0.16 nT then remains in the offset term.

[19] Because there does not appear to be a physical reason for the annual variation, we suggest that it might be an artifact of the location of magnetometers that are used in the *Dst* calculation. There are three stations in the Northern Hemisphere but only one in the Southern Hemisphere. The *Dst* index may respond more to pressure enhancements near the summer solstice than during the winter solstice because during the summer solstice the Northern Hemisphere stations are oriented toward the dayside magnetopause where the magnetopause currents are largest. Likewise the tilt of the magnetosphere may distort the outer portion of the magnetosphere and thus the ring current represented by the dst1 term. A discussion and further references concerning the annual variation are given by *Mursula and Karinen* [2005]. They also attribute and display evidence that the annual variation is due to the asymmetry in the number of magnetometer stations in the Northern and Southern Hemispheres but attribute the effect to a seasonal shift in the ionospheric Sq current system.

3. Results and Discussions

[20] An example of how these terms add to produce the predicted *Dst* and a comparison with the "Kyoto *Dst*" is shown in Figure 2. It is evident that the modeled *Dst* captures the variations of "Kyoto *Dst*" well, during both storms as well as during quiet times. One can also see that different *dst* terms have different decay rates and the *dst*2 term, which may be interpreted as the partial ring current, can make comparable contributions as *dst*1 term, which

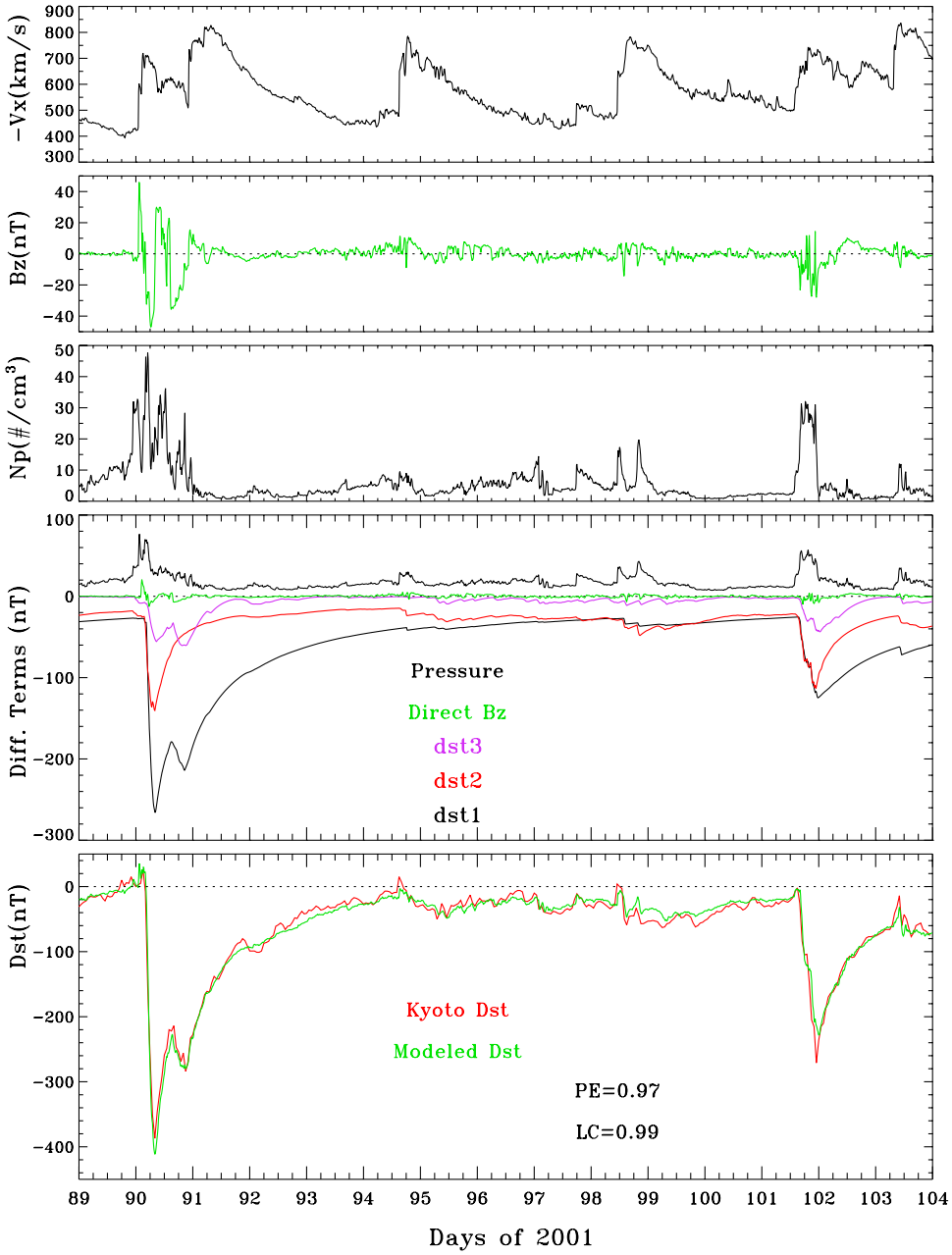

Figure 2. The most relevant solar wind parameters (top three panels) and the contributions from the different terms in the *Dst* model, the predicted *Dst*, and "Kyoto *Dst*" index, for 15 days in 2001 (30 March to 14 April). This period had the largest magnetic storm in terms of the *Dst* since the −589 nT magnetic storm of 14 March 1989.

may be interpreted as the main ring current, during the main phase of the storm. This is consistent with a recent study by *Liemohn et al.* [1999].

[21] For the selected period, the PE is 0.97 and LC is 0.99. The PE is high for this period even though the predicted *Dst* overshot the magnitude of the first storm because of the large variance in *Dst* during this period. The prediction efficiency is higher for active periods because, as discussed later, an unpredictable diurnal variation dominates the error during quiet periods.

[22] Figure 3 shows scatterplots of the predicted *Dst* versus "Kyoto *Dst*" for the years 1995–2002. About 4% of the solar wind data is missing owing to either Wind perigee passes or other missing data or unreliable measurements (including 14–15 July 2000 event). We do not include these data gaps in our modeling. One can see that there were no magnetic storms during the years 1995–1999 with *Dst* below −250 nT, while there were such large magnetic storms during 2000–2001 (also shown in Figure 4). For each year, the predicted *Dst* and the measured *Dst* are well correlated, demonstrated by the closely clustered points, though with varying PE and LC (listed on each panel). For the whole 8 years, 1995–2002, the PE is 0.914 and LC is 0.956.

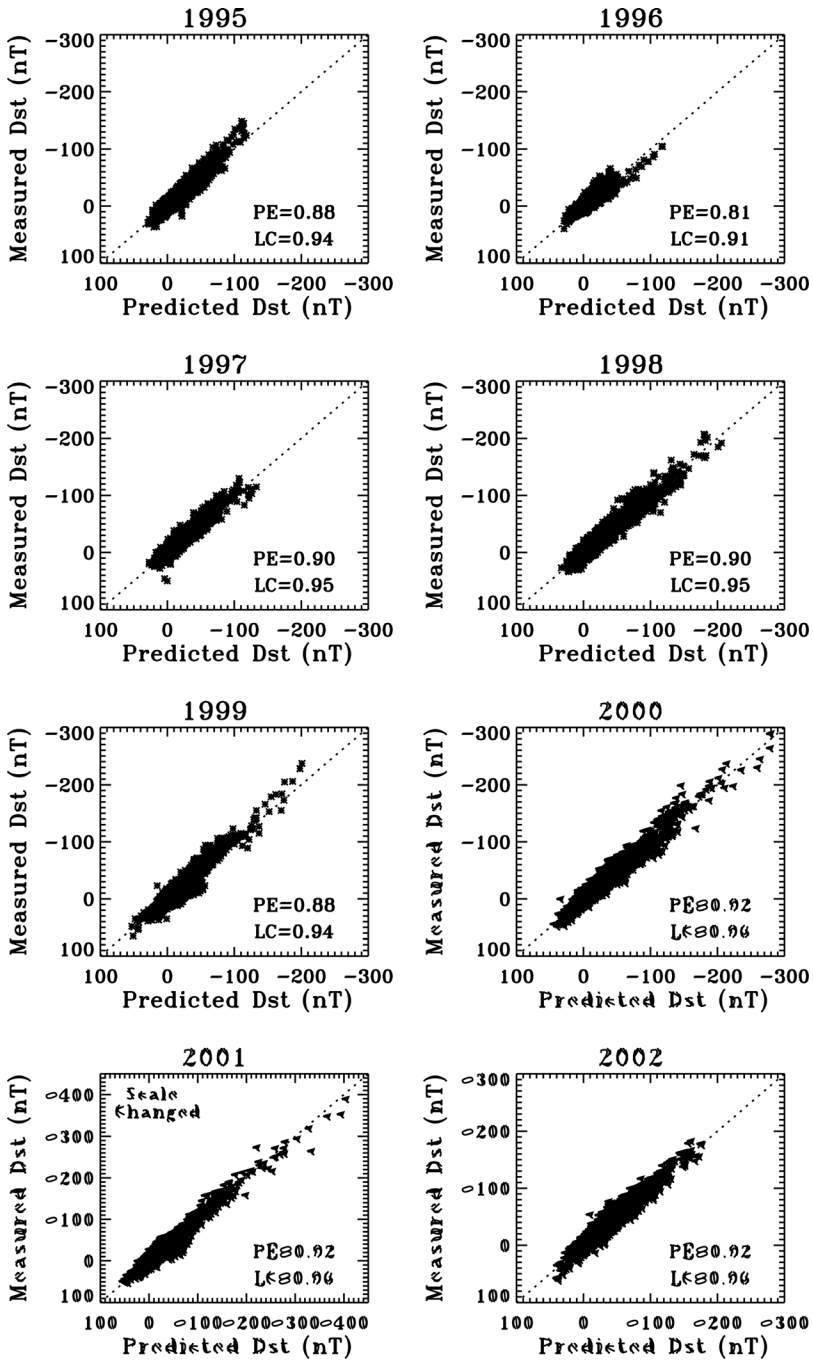

Figure 3. Scatterplot of predicted *Dst* versus "Kyoto *Dst*" for the years 1995–2002. Here 4% of the hourly *Dst* values have been removed because of gaps in the solar wind data.

[23] Some outlier points are worth noting. The outlier points for 1997 near the predicted *Dst* value of zero are due to inaccurate measurements of the solar wind density. A very dense, cold solar wind plasma, ~180 ions/cm^3 [*Larson et al.*, 2000], enveloped the Earth during the recovery phase of the famous 10 January 1997 magnetic storm and coronal mass ejection event and produced a positive *Dst* of 50 nT. The model failed to predict fully the positive excursion because the solar wind density used in the "pressure term" in the model was only 67 ions/cm^3, as provided by the 3D plasma/energetic particle instrument on WIND [*Lin et al.*, 1995], which does not function well for such extreme cold, dense, solar wind plasma conditions.

[24] Of special interest are large storms. Figure 4 shows a comparison of the predicted *Dst* with the "Kyoto *Dst*" for the six largest magnetic storms of 1995–2002 for which good solar wind measurements are available. We would like to note again that these examples are portions of a single comparison covering 8 years and no parameters were changed to optimize the prediction for any one storm. For each storm period, the predicted *Dst* tracks the "Kyoto *Dst*"

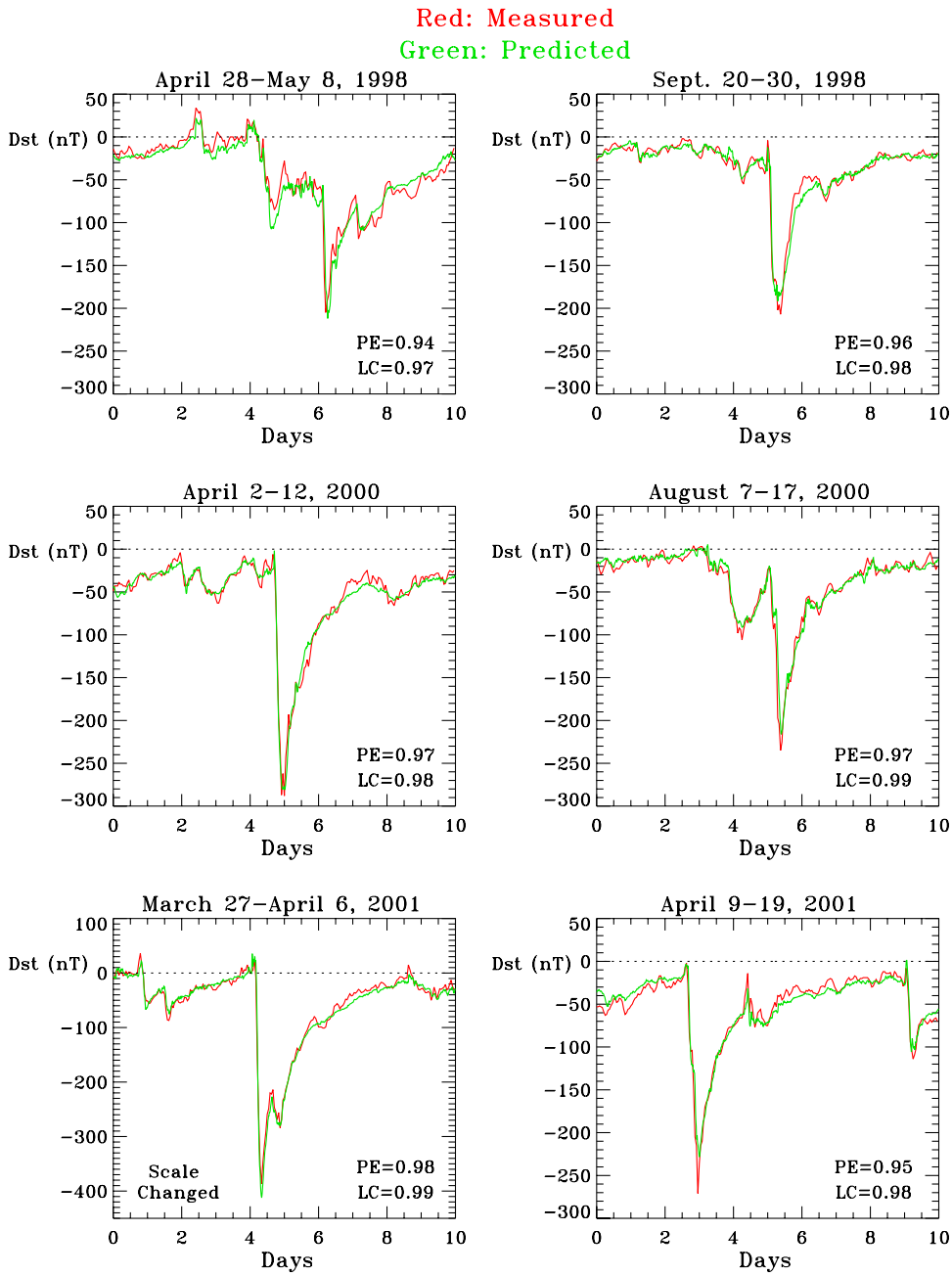

Figure 4. Comparison of the predicted *Dst* with the "Kyoto *Dst*" for the largest magnetic storms for which good solar wind measurements were available during the 1995–2002 period.

well. PE and LC (listed on each panel) vary between 0.94–0.98 and 0.97–0.99, respectively, for these six periods.

[25] Several sources of error in the *Dst* prediction were discussed previously [*Temerin and Li*, 2002]. Here we discuss one of the more important and obvious sources in more detail. Ideally, *Dst* should be a measure of the perturbation in the magnetic field at the center of the Earth's dipole magnetic field due to magnetospheric currents. In practice, the measured magnetic field is affected by ionospheric currents from the so-called quiet-time ionospheric Sq current system, which leads to large diurnal variations in the magnetometer data. Much of this diurnal variation is removed before *Dst* is calculated by averaging the diurnal variations for each station each month during four of the magnetically quietest days of the month and then subtracting this average variation from the other days [*Sugiura and Kamei*, 1991]. However, this procedure is not completely satisfactory since the "diurnal" variation varies from day to day (that is to say, the Sq current system is only nominally diurnal), and because even during quiet days there is some real magnetospheric current variation which may then also be subtracted from the other days and thus introduce an additional error.

[26] The effect of some of this error on the *Dst* prediction is shown in Figure 5, which shows the autocorrelation of the *Dst* data (the upper curve) and of the error in the model

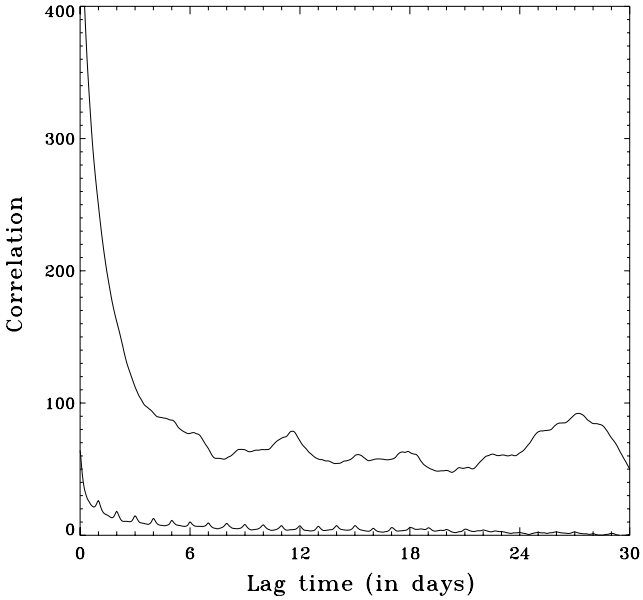

Figure 5. Autocorrelation of the *Dst* data (the upper curve) and of the error in the model (lower curve) as a function of time lag in days for the years 1995–2002.

(lower curve) as a function of time lag in hours for the years 1995–2002. The zero lag point of the lower curve is equivalent to the mean square error. The 27-day peak in the *Dst* autocorrelation no doubt reflects the solar rotation period. While the diurnal periodicity in *Dst* is barely noticeable, it is quite obvious in the autocorrelation of the error in the *Dst* prediction as seen in the diurnal periodicity of the lower curve in Figure 5. By extrapolating the periodic portion of the signal to zero time lag, we can estimate that about 25% to 30% of the mean square error in our model prediction is due to the unremoved periodic portion of the Sq current system. This error is not removable if one bases predictions of *Dst* solely on the solar wind because the amplitude and phase of the error vary. This error tends to dominate during periods of quiet magnetic activity and is one reason active times have a greater PE.

[27] Magnetospheric activity should also have a diurnal variation for the same reason that it has a seasonal variation: Magnetospheric activity is controlled, in part, by the angle of the magnetic dipole with respect to the solar wind flow direction. This angle varies diurnally as well as seasonally because of the offset of the magnetic dipole with respect to the rotation axis of the Earth. However, as noted in our previous paper [*Temerin and Li*, 2002], the diurnal variation is smaller than would be expected from the magnitude of the seasonal variation. In this updated model we have allowed the phase of the diurnal variation for each of the terms of the model to vary independently. This has increased the average diurnal variation of each term but because the terms now add up out of phase the overall diurnal variation in the model remains small. This small and inconsistent behavior of the diurnal variation in the model is likely due, in part, to the subtraction of much of the diurnal variation from the *Dst* index, which is done to eliminate the effects of the ionospheric Sq current system but may also eliminate much of the true magnetospherically caused diurnal variation. Since our model tries to match the *Dst* index, it cannot reproduce the true magnetospheric diurnal variation.

[28] Another way to look at the prediction error is as a function of magnetospheric activity. Figure 6 shows the PE and RMS prediction error as a function of *Dst*. The figure shows that for large magnitudes of *Dst*, the error is approximately proportional to *Dst* while the PE asymptotes to 0.99. The figure can be interpreted that the error consists of two parts: a base error of about 6 nT that doesn't depend on magnetic activity and which is probably due mostly to the Sq current system and an error whose RMS value is about 10% of *Dst*. In terms of the variance of the error as a function of *Dst* we get approximately

$$\text{RMS error} = \sqrt{(\text{variance error})} = \sqrt{\left[6.0^2 + (0.1 * Dst)^2\right]},$$

which means that except for the base error of 6 nT the prediction efficiency is approximately 0.99 ($1-0.1^2$).

[29] One of our main motivations in trying to predict *Dst* had been to determine the predictability of magnetospheric activity. If the above assumptions are approximately correct, the PE for actual magnetospheric activity is close to 0.99 or very high. This means that the magnetosphere is a very predictable system for the large-scale currents that influence *Dst*.

[30] We are using our *Dst* model to make near real-time predictions of the *Dst* index (and also the daily averaged >2 MeV electron flux at geosynchronous orbit [*Li et al.*, 2001b; *Li*, 2004]) based on data from the ACE satellite. The results are currently available in real-time at http://lasp.colorado.edu/~lix. Also available on the web site is a monthly archive of model predictions starting from 1995. Near real-time predictions are based on preliminary data from the ACE satellite and are compared with the quick-look *Dst* index. Both the quick-look *Dst* index and the preliminary ACE data can differ substantially from their final versions. The model is based on the level 2 (that is, final) versions of the satellite data and the final version of "Kyoto *Dst*."

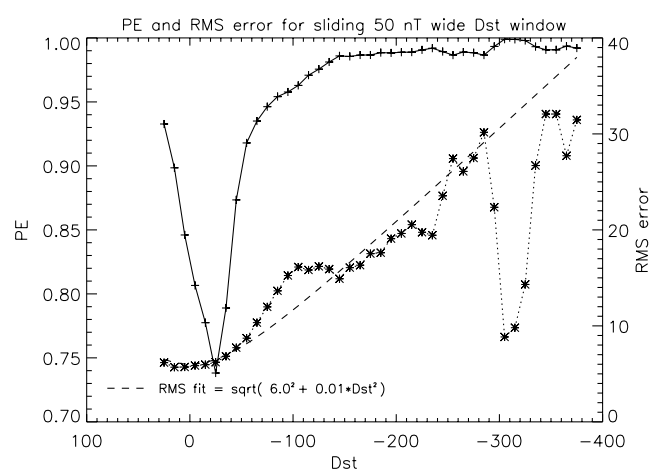

Figure 6. Prediction efficiency (PE, + sign) and the RMS error (asterisks) of the model as a function of the measured *Dst* for a 50-nT-wide sliding window centered on the respective points.

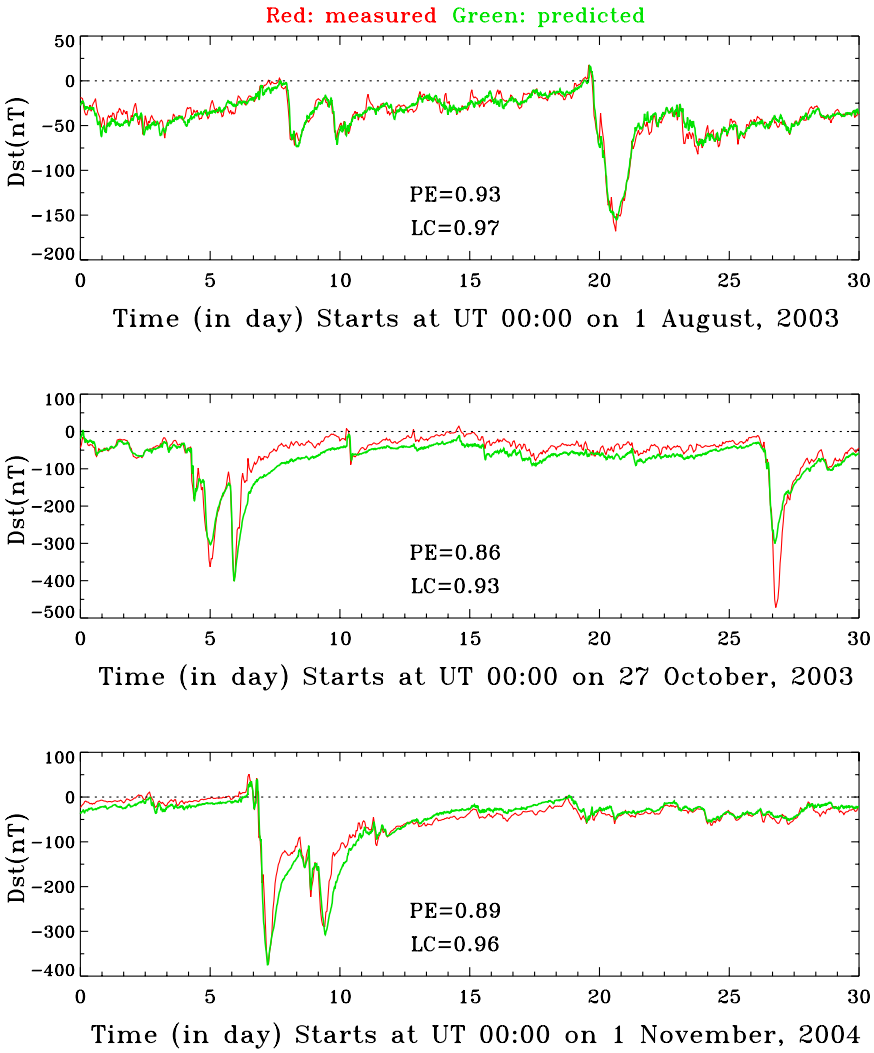

Figure 7. Three examples of out-of-sample comparisons between our model prediction and the provisional version of the "Kyoto *Dst*" index from 2003 and 2004. No model parameters were changed to produce the predicted results except that the offset term was set to a constant.

[31] Figure 7 shows three examples of out-of-sample comparisons between our model (except that the offset term is just a constant) and the provisional version of the "Kyoto *Dst*" index from 2003 and 2004. The top panel shows relatively good agreement between the model and the provisional version of the "Kyoto *Dst*" index. The middle panel shows the two largest magnetic storms of the current solar cycle, the so-called Halloween storm of 2003 and the magnetic storm of 20–21 November 2003. The Halloween storm had the largest solar wind velocity of the solar cycle, over 2000 km/s, and the 20 November event was the largest magnetic storm of the solar cycle as measured by *Dst* (−472 nT according to the provisional values). The bottom panel presents a comparison of the model for the largest magnetic storm of 2004. The biggest discrepancy in our modeled results for the years 1995–2005 is 20 November 2003. Our model gives about −300 nT versus −472 nT for the provisional *Dst* index. It is unlikely that this discrepancy is due to the use of the provisional rather than the final *Dst* index. Past comparisons between the provisional and final *Dst* suggest differences of the order of 10 nT between these versions of the *Dst* index and thus relatively small percentage differences for larger storms.

[32] A slightly earlier version of this model was used to model the largest (allegedly) magnetic storm ever recorded: the Carrington storm of 1–2 September 1859, which may have had an equivalent *Dst* value of below −1500 nT [*Tsurutani et al.*, 2003]. The results show that such a large negative *Dst* value is possible within the context of the model as long as there is sufficiently fast solar wind (∼1600 km/s) and a very large and long-lasting negative IMF Bz (∼−60 nT for a couple of hours) [*Li et al.*, 2006].

4. Summary

[33] The main overall goal of our research into *Dst* has been to determine the predictability of the magnetosphere given a solar wind driver. We have shown that the magnetosphere is highly predictable in terms of the large-scale currents that influence *Dst*. Another more technical goal of this article is to provide an update of our previous *Dst* prediction model as described in the Appendix A. We have

updated the parameters in the model, improved the model's behavior for more extreme values of the solar wind, and experimented with some new terms. The motivation for the new terms is partly to improve the model but also to explore the physical behavior of the magnetosphere. For instance, we added the annual modulations in the model to determine the source of the annual variation of *Dst*. We added a dependence on the previous values of Bz in the driver terms to test models (see Appendix A) that show that super-dense plasmasheets enhance subsequent magnetic storms [*Thomsen et al.*, 2003]. Though the result was somewhat ambiguous as far as the motivating question is concerned, the Bz terms did reduce the error in the model by about 1%. Our *Dst* model suggests that there are three current systems within the magnetosphere which affect the surface magnetic field of the Earth. Our model also has an IMF Bz contribution as though a portion of the IMF penetrates directly to the surface of the Earth, a pressure term, and an offset term. For this 8-year period, the linear correlation between the model and the *Dst* index is 0.956, the prediction efficiency is 0.914, and the RMS error of the prediction is 6.65 nT. An analysis of some of the error in the model indicate that at least 25% of the remaining error is due to the effect on the *Dst* index of a portion of the Sq ionospheric current system. A further analysis of the error indicates that close to 99% of the variance in the large-scale currents that influence *Dst* are predictable. An examination of the model's behavior for the six largest magnetic storms during 1995–2002 for which there is good solar wind data shows excellent agreement with the *Dst* index. It was shown that the annual variation in the *Dst* index is mainly due to magnetopause and ring currents. The dependence of the model on the solar wind implies that magnetospheric activity depends on the solar wind approximately in proportion to the square root of the density, square of the velocity, and linearly with the magnetic field of the solar wind. In addition, the model shows that there is a strong dependence on the direction of IMF such that magnetic activity depends approximately on the sixth power of the sine of half the IMF clock angle and a seasonal dependence that depends on the angle between the dipole axis of the Earth and the solar wind velocity.

Appendix A

[34] Here we describe the terms in the model *Dst* and how these terms have changed from our previous model. The model *Dst* is calculated as a sum of six terms:

$$Dst = dst1* + dst2* + dst3* + (pressure\ term)* + (direct\ Bz\ term)* + (offset\ term).$$

The terms *dst*1, *dst*2, *dst*3, (*pressure term*), and (*direct Bz term*) were in our previous model. The terms *dst*1*, *dst*2*, *dst*3*, (*pressure term*)*, (*direct Bz term*)* differ, in part, in that they incorporate an annual variation as follows:

$$\begin{aligned} dst1* &= dst1 \cdot (1.0 + 0.0807 \sin(t \cdot fy + 1.886)), \\ dst2* &= dst2 \cdot (1.0 + 0.0251 \sin(t \cdot fy + 3.18)), \\ dst3* &= dst3 \cdot (1.0 + 0.0901 \sin(t \cdot fy + 5.31)) \\ &\quad \cdot (1 - 0.00007 \cdot dst1*), \\ (direct\ Bz)* &= (direct\ Bz) \\ &\quad \cdot (1.0 + 0.293 \sin(t \cdot fy + 3.19)) \\ &\quad \cdot (1 + 0.0034 \cdot dst1*), \\ (pressure)* &= (pressure) \\ &\quad \cdot (1.0 + 0.0986 \sin(t \cdot fy - 1.383)) \\ &\quad \cdot (1 + 0.00184 \cdot dst1*), \end{aligned}$$

where $fy = 2\pi/365.24$ and t is the time in days from 1995. The annual variation had previously been incorporated as part of the offset term. While the offset term still has some annual variation, it is now much smaller (an amplitude of 0.158 nT versus 1.44 nT previously for the years 1995–1999 and about 3.2 nT for the years 1995–2002 if the annual variation is not incorporated into the individual terms). The largest contribution to the annual variation comes from the pressure term with the dst1 term also making a significant contribution. (Note that because dst1 is negative and the pressure is positive, their contributions are in phase.) The other terms are smaller and of different phase. The overall effect is to produce an annual variation that is positive near the Northern Hemisphere summer solstice. In the absence of a physical mechanism to explain the annual variation, our so far untested working hypothesis is that it is due to the north-south hemispheric asymmetry in the number of magnetic observatories used to calculate *Dst* (three in the Northern Hemisphere and one in the Southern Hemisphere) together with the hemispherical asymmetries in the magnetospheric current systems caused by the seasonal tilt of the dipole with respect to the solar wind velocity.

[35] We also experimented with including a dst1 modulation on the other terms. Since the dst1 term represents the main ring current one could imagine that the effect of solar wind pressure or the effect of the other magnetospheric current systems would be different if there is a large ring current. However, the addition of these terms makes only a small improvement in the model. For instance the current form of the pressure term implies that if the dst1* term is −100 nT, the effect of the solar wind pressure on increasing *Dst* is reduced by 18.4%.

[36] Now we describe the terms *dst*1, *dst*2, *dst*3, (*pressure term*), (*direct Bz term*) and the *offset term*.

$$\begin{aligned} dst1(t + dt) = dst1(t) &+ \{5.041 \cdot 10^{-3} \cdot [-dst1(t)]^{2.017} \\ &\cdot (1 + \mathrm{erf}(-0.010 b_z)) + fe1(t) \\ &\cdot [1 + \mathrm{erf}(-0.0094 b_z(t - 0.0486) \\ &- 0.0118 b_z(t - 0.181) + 0.0138 b_z(t - 0.271))] \\ &\cdot \exp(0.00313 dst1(t - 0.132) \\ &+ 0.01872 dst2(t - 0.0903))\} dt. \end{aligned} \tag{A1}$$

[37] In words this equation says that dst1 at the current time step is equal to dst1 at the previous time step plus a nonlinear decay term that depends on the magnitude of dst1 and weakly on IMF Bz plus a growth term that is mostly given by fe1. The factor fe1 depends on solar wind parameters and has a modulation that depends on the values of dst1, dst2, and the IMF Bz previously. The modulation of the growth by the previous values of dst1 and dst2 was in our previous model. However, here the terms are within an

exponential. Thus, for large negative previous values of dst1 and dst2 (dst1 and dst2 are always negative terms), the growth can approach zero but doesn't change sign as it could previously. The terms involving the previous values of the IMF Bz were put in to test the hypothesis that dense plasmasheets should lead to a larger magnetic storm [*Thomsen et al.*, 2003]. Though our model uses only solar wind parameters, it has been found that dense plasmasheets are associated with a positive IMF Bz. Thus there could be an association between the previous value of the IMF Bz and the strength of magnetic storms. We find (i.e., equation (A1), shows) that the dst1 term growth rate (i.e., the main ring current) would be enhanced if the IMF Bz is instead negative rather and positive 70 min (0.0486 days) and 260 min (0.181 days) prior but is enhanced if the IMF is positive 390 min (0.271 days) prior to the current time. The Bz factor in the decay rate was put in to test for its possible effect on the decay. It has only a small effect here.

$$\begin{aligned} dst2(t+dt) = dst2(t) + \Big\{ & 0.00955[-dst2(t)]^{2.017} \\ & \cdot (1+\mathrm{erf}(-0.014b_z)) + df2(t) \\ & \cdot [1+\mathrm{erf}(-0.0656b_z(t-0.0625) \\ & + 0.0627b_z(t-0.104))] \\ & \cdot \exp(0.01482dst1(t-0.264))\Big\}dt \end{aligned} \tag{A2}$$

$$\begin{aligned} dst3(t+dt) = dst3(t) + \Big\{ & 5.10(-dst3(t))^{0.952} \\ & \cdot (1+\mathrm{erf}(-0.027b_z(t))) + df3(t) \\ & \cdot [1+\mathrm{erf}(-0.0471b_z(t-0.0278) \\ & + 0.0184b_z(t-0.139))]\Big\}dt. \end{aligned} \tag{A3}$$

[38] The forms of the dst2 and dst3 equations are similar to that of dst1 and were modified from their previous versions in a similar manner. The dst2 term depends on the previous value of dst1 but not dst2. The dst3 term does not depend on previous values of dst1 or dst2. The modulations of the driver term on the previous values of the IMF Bz have different magnitudes and time delays but the pattern is similar to that of the dst1 term: the more recent values of negative IMF Bz enhance the driver term.

$$\begin{aligned} fe1(t) = & -1.703\cdot 10^{-6}\big(1.+\mathrm{erf}\big(-0.09b_p\cdot\cos(\beta-0.015)\cdot dh\big)\big) \\ & \cdot tst3\cdot[(exx-1231.2/tst4+abs(exx-1231.2/tst4)) \\ & +(exx-3942/tst4+abs(exx-3942/tst4))] \\ & \cdot v_x^{1.307}n^{0.548}. \end{aligned}$$

[39] The form of the fe1 was altered by the addition of the error function. See the comment on the fe2 term for the rational for this alteration.

$$\begin{aligned} & b_p = \left(b_y^2+b_x^2\right)^{\frac{1}{2}}, \\ & dh = 0.0435\cos(fy\cdot t+0.1680) - 0.0208\sin(2\pi\cdot t-1.589), \\ & \beta = \mathrm{atan}(bx, by), \\ & exx = v_x\cdot b_t^{0.993}\sin^{7.29}(\theta), \\ & \theta = -\left(acos\left(-\frac{b_z}{b_t}\right)-\pi\right)/2, \\ & b_t = \left(b_y^2+b_z^2\right)^{\frac{1}{2}}, \\ & tst3 = \left[\left(1-\cos^2(\phi)\right)^{\frac{1}{2}}/0.95097\right]^{-0.13}, \\ & tst4 = \left[\left(1-\cos^2(\phi)\right)^{\frac{1}{2}}/0.95097\right]^{6.54}, \end{aligned}$$

$$\begin{aligned} \cos(\phi) = & 0.1635\sin(t\cdot fy+0.0449)\cdot\sin(2\pi t-t\cdot fy-1.632) \\ & +\cos(t\cdot fy+0.0449)\cdot(0.39+0.178 \\ & \cdot\cos(2\pi t-t\cdot fy-1.632)), \end{aligned}$$

$$\begin{aligned} & df2 = 1440.0\cdot tst7\cdot fe2/(-fe2+922.1), \\ & fe2 = 5.172\cdot 10^{-8}\cdot exx2 \\ & \quad\cdot\big(1.+\mathrm{erf}\big(0.418b_p\cdot\cos(\beta-0.015)\cdot dh\big)\big). \end{aligned}$$

[40] The fe2 and fe3 terms were modified by enclosing what is now the argument of the error function by the error function. Previously, for large values of IMF bp (essentially IMF By), the denominator in the expression for df2 and df3 could become zero. The error function for the fe1 term was introduced to have consistent forms for similar terms.

$$\begin{aligned} & exx2 = n^{0.493}\cdot v_x^{2.955}\cdot b_t^{1.105}\sin^{5.24}(\theta), \\ & tst7 = \left[\left(1-\cos^2(\phi_7)\right)^{\frac{1}{2}}/0.95097\right]^{2.84}, \end{aligned}$$

$$\begin{aligned} \cos(\phi_7) = & 0.1635\sin(t\cdot fy+0.0449)\cdot\sin(2\pi t-t\cdot fy-0.79) \\ & +\cos(t\cdot fy+0.0449)\cdot(0.39+0.178\cdot\cos(2\pi t-t\cdot fy \\ & -0.79)). \end{aligned}$$

[41] The cos(phi) terms (what is now cos(phi), cos(phi7), cos(phi8), cos(phi5), cos(phi6)) were previously all the same. They differ now because the phase that affects the diurnal variation of the various terms is different. The six terms in our model (dst1, dst2, etc) have an annual and, except the offset term, a diurnal variation. The annual variation is a function of the angle between the magnetic dipole of the Earth and the solar wind velocity and has both an annual and a diurnal variation. Previously we found from the best fit that the magnitude of the diurnal variation was not consistent with the magnitude of the annual variation. This may be due, in part or in whole, to the fact that a diurnal effect is subtracted from the Dst index in order to reduce the effect of Sq ionospheric current system on the *Dst* index. Such a subtraction can also affect the diurnal variation due to magnetospheric effects. Also the dipole tilt that produces the annual variation can also effect the diurnal variation. Thus, to further explore these diurnal affects, we let the diurnal phase of the various terms be independent.

$$\begin{aligned} & df3(t) = 272.9\cdot tst8\cdot fe3/(-fe3+60.5), \\ & fe3 = -0.0412\cdot exx3\cdot\big(1.+\mathrm{erf}\big(1.721b_p\cdot\cos(\beta-0.015)\cdot dh\big)\big), \\ & exx3 = n^{0.397}\cdot v_x^{0.576}\cdot b_t^{1.413}\sin^{8.56}(\theta), \\ & tst8 = \left[\left(1-\cos^2(\phi_8)\right)^{\frac{1}{2}}/0.95097\right]^{2.49}, \end{aligned}$$

$$\cos(\phi_8) = 0.1635\sin(t\cdot fy + 0.0449)\cdot\sin(2\pi t - t\cdot fy - 2.81) + \cos(t\cdot fy + 0.0449)\cdot(0.39 + 0.178 \cdot\cos(2\pi t - t\cdot fy - 2.81)),$$

$$direct\ B_z\ term = 0.574\cdot tst5\cdot b_z \quad \text{(A4)}$$

where $tst5 = [(1\text{-}\cos^2(\phi_5))^{\frac{1}{2}}/0.95097]^{5.13}$,

$$\cos(\phi_5) = 0.1635\sin(t\cdot fy + 0.0449)\cdot\sin(2\pi t - t\cdot fy + 0.27) + \cos(t\cdot fy + 0.0449)\cdot(0.39 + 0.178\cdot\cos(2\pi t - t\cdot fy + 0.27)),$$

$$(pressure\ term) = \left[0.330\cdot b^2\cdot(1. + 0.100n) + \left(1.621\cdot 10^{-4}\cdot tst6\cdot v^2 + 18.70\right)\cdot n\right]^{\frac{1}{2}}. \quad \text{(A5)}$$

[42] The pressure term is the square root of weighted sum of the following terms: b^2, nb^2, nv^2, and n. The nv^2 term is the dynamic pressure and provides the main contribution and, in most theoretical considerations, the only contribution to the pressure. However, we have that separating the terms in this improves the prediction efficiency though we don't have good explanation for it. In our previous model, we did not have the b^2*n term.

$$tst6 = \left[\left(1 - \cos^2(\phi_6)\right)^{\frac{1}{2}}/0.95097\right]^{-2.44}$$

$$\cos(\phi_6) = 0.1635\sin(t\cdot fy + 0.0449)\cdot\sin(2\pi t - t\cdot fy - 0.21) + \cos(t\cdot fy + 0.0449)\cdot(0.39 + 0.178 \cdot\cos(2\pi t - t\cdot fy - 0.21)).$$

[43] The offset term for the years 1995–1999 is

$$offset = 11.70 + 0.158\sin(t\cdot fy - 0.94) - 0.00954\cdot t + 8.159\cdot 10^{-6}\cdot t^2. \quad \text{(A6)}$$

The offset term for the years 2000–2002 is

$$offset = 19.35 + 0.158\sin(fy\cdot tt - 0.94) + 0.01265\cdot tt - 2.224\cdot 10^{-5}\cdot 10^{-6}\cdot tt^2, \quad \text{(A7)}$$

where tt is the time in days starting from the beginning of 2000.

[44] The offset term is shown is Figure 1. Because we did two separate quadratic fits for the years 1995–1999 and the years 2000–2002, there is a discontinuity at the end of 1999.

[45] The solar wind data are first averaged to 10-min intervals at spacecraft's positions and then ballistically propagated to the Earth using the solar wind velocity and the upstream distance of WIND or ACE. In the case of WIND the actual upstream distance is used; in the case of ACE, the upstream distance is assumed to be 238.6 R_E. After propagating to the Earth, the data are then interpolated to 10-min intervals to be used as input to the *Dst* model.

[46] The dst1, dst2, dst3, pressure term, direct IMF Bz term, and offset terms are added (after interpolation) with time delays of 5.3, −14.6, 30.2, −1.6, 23.1, and 5.3 min, respectively, and then smoothed over 50 min for comparison with the "Kyoto *Dst*."

[47] **Acknowledgments.** We appreciate the effort by the science teams (WDC for Geomagnetism, Kyoto, Wind/3D, Wind/Mag, ACE/SWEPAM, ACE/Mag) for making the data available. We thank S. Monk of LASP for programming efforts. This work was supported by NASA grant (NAG5-13518) and NSF grants (CISM and ATM-0233302).

[48] Arthur Richmond thanks Hualiang Wei and two other reviewers for their assistance in evaluating the paper.

References

Burton, R. K., R. L. McPherron, and C. T. Russell (1975), An empirical relationship between interplanetary conditions and *Dst*, *J. Geophys. Res.*, *80*, 4204.

Cliver, E. W., Y. Kamide, and A. G. Ling (2000), Mountains versus valleys: Semiannual variation of geomagnetic activity, *J. Geophys. Res.*, *105*, 2413.

Karinen, A., and K. Mursula (2005), A new reconstruction of the *Dst* index for 1932–2002, *Ann. Geophys.*, *23*, 475.

Larson, D. E., R. P. Lin, and J. Steinberg (2000), Extremely cold electrons in the January 1997 magnetic cloud, *Geophys. Res. Lett.*, *27*, 157.

Lepping, R. P., et al. (1995), The Wind magnetic field investigation, *Space Sci. Rev.*, *71*, 207.

Li, X. (2004), Variations of 0.7–6.0 MeV electrons at geosynchronous orbit as a function of solar wind, *Space Weather*, *2*(3), S03006, doi:10.1029/2003SW000017.

Li, X., D. N. Baker, S. G. Kanekal, M. Looper, and M. Temerin (2001a), Long-term measurements of radiation belts by SAMPEX and their variations, *Geophys. Res. Lett.*, *28*, 3827.

Li, X., M. Temerin, D. N. Baker, G. D. Reeves, and D. Larson (2001b), Quantitative prediction of radiation belt electrons at geostationary orbit based on solar wind measurements, *Geophys. Res. Lett.*, *28*, 1887.

Li, X., M. Temerin, B. T. Tsurutani, and S. Alex (2006), Modeling of 1–2 September 1859 super magnetic storm, *Adv. Space Res.*, doi:10.1016/j.asr.2005.06.070, in press. (Available at http://www.sciencedirect.com)

Liemohn, M. W., J. U. Kozyra, G. V. Khazanov, M. F. Thomsen, and T. E. Clayton (1999), Analysis of the early phase ring current recovery mechanisms during geomagnetic storms, *Geophys. Res. Lett.*, *26*, 2845.

Lin, R. P., et al. (1995), A three-dimensional plasma and energetic particle investigation for the Wind spacecraft, *Space Sci. Rev.*, *71*, 125.

McComas, D. J., et al. (1998), Solar Wind Electron Proton Alpha Monitor (SWEPAM) for the Advanced Composition Explorer, *Space Sci. Rev.*, *86*, 563.

Mursula, K., and A. Karinen (2005), Explaining and correcting the excessive semiannual variation in the *Dst* index, *Geophys. Res. Lett.*, *32*, L14107, doi:10.1029/2005GL023132.

Perreault, P., and S.-I. Akasofu (1978), A study of geomagnetic storms, *Geophys. J. R. AstrON. Soc.*, *54*, 547.

Siscoe, G. L., G. M. Erickson, B. U. Sonnerup, N. C. Maynard, J. A. Schoendorf, K. D. Siebert, D. R. Weimer, W. W. White, and G. R. Wilson (2002), Hill model of transpolar potential saturations: Comparisons with MHD simulations, *J. Geophys. Res.*, *107*(A6), 1075, doi:10.1029/2001JA000109.

Smith, C. W., et al. (1999), The ACE Magnetic Field Experiment, *Space Sci. Rev.*, *86*, 613.

Sugiura, M., and T. Kamei (1991), Equatorial *Dst* index 1957–1986, *IAGA Bull. 40*, ISGI Publ. Off., Saint-Maur-des-Fosses, France.

Temerin, M., and X. Li (2002), A new model for the prediction of *Dst* on the basis of the solar wind, *J. Geophys. Res.*, *107*(A12), 1472, doi:10.1029/2001JA007532.

Thomsen, M. F., J. E. Borovsky, R. M. Skoug, and C. W. Smith (2003), Delivery of cold, dense plasma sheet material into the near-Earth region, *J. Geophys. Res.*, *108*(A4), 1151, doi:10.1029/2002JA009544.

Tsurutani, B. T., W. D. Gonzalez, G. S. Lakhina, and S. Alex (2003), The extreme magnetic storm of September 1–2, 1859, *J. Geophys. Res.*, *108*(A7), 1268, doi:10.1029/2002JA009504.

X. Li, Laboratory for Atmospheric and Space Physics, University of Colorado, 1234 Innovation Drive, Boulder, CO 80303-7814, USA. (lix@lasp.colorado.edu)

M. Temerin, Space Sciences Laboratory, University of California, Berkeley, CA 94720, USA. (temerin@mac.com)